Astron. Astrophys. 321, 557–567 (1997)

ASTRONOMY
AND
ASTROPHYSICS

Two-fluid models for stationary dust driven winds

II. The grain size distribution in consideration of drift

D. Krüger and E. Sedlmayr

Institut für Astronomie und Astrophysik, PN 8-1 Hardenbergstraße 36, D-10623 Berlin, Germany

Received 13 January 1996 / Accepted 24 October 1996

Abstract. A multi-component method for the description of the evolution of the grain size distribution in consideration of a size dependent grain drift and growth rate is applied in order to model dust driven winds around cool C-stars.

Grain drift introduces several modifications concerning dust growth: On the one hand the residence time in the region of efficient growth is reduced, on the other hand the growth efficiency is higher due to an increased collisional rate. For carbon grains the surface density of radical sites is increased, but on the other hand there is a reduction of the sticking efficiency of the growth species for drift velocities larger than $\sim 5\,\mathrm{km\,s^{-1}}$. Furthermore, nonthermal sputtering may become relevant for high drift velocities.

It is found that the consideration of drift results in a considerable distortion of the size distribution as compared to the case of zero drift velocity. Generally, there are less, but larger grains if drift is included.

Key words: stars: mass loss – circumstellar matter – stars: AGB – stars: carbon – hydrodynamics

1. Introduction

It now seems to be well established that dust is an important component of the extended atmospheres around late-type stars. A wealth of papers has been devoted to the investigation of the hydro- and thermodynamical role of dust in the circumstellar environment (see, e.g. the reviews of Lafon & Berruyer 1991, Sedlmayr & Dominik 1995 and references therein).

Although the art of modeling circumstellar dust shells (CDS) is very advanced and includes an elaborate treatment of time-dependent hydrodynamics (Bowen 1988, Fleischer et al. 1992), non-equilibrium chemistry (Nejad & Millar 1987, Beck et al. 1992), dust formation (Kozasa et al. 1984, Gail & Sedlmayr 1988), and radiative transfer (Rowan-Robinson & Harris 1982, Winters et al. 1994) the majority of models for CDS is lacking a proper treatment of grain drift.

Those models including grain drift rather concentrate on aspects such as the momentum coupling of grains to the bulk of the gas (MacGregor & Stencel 1992, Krüger et al. 1994), the dynamical dilution of the dust component (Netzer & Elitzur 1993, Krüger et al. 1994) or the frictional heating due to drifting dust particles (Tielens 1983, Krüger et al. 1994).

Concerning the growth and nonthermal sputtering of drifting dust grains in circumstellar envelopes a first investigation was made by Kwok (1975). However, in his work all grains were assumed to have a uniform if time-dependent radius.

In contrast, Dominik et al. (1989) determined the entire distribution of grain sizes in self-consistent models for dust driven winds. In these models dust formation and growth were treated explicitly assuming, however, negligible drift and a dust growth rate independent of the grain size. Although the mere *effects* of drift on grain growth have already been investigated by Dominik et al. (1989) their method does not allow for a self-consistent treatment of these effects nor of nonthermal sputtering.

It is the aim of this paper to expand these preliminary investigations by means of a general and self-consistent modeling procedure. We are specifically interested in how far drift motion influences the formation and growth of dust particles in stellar winds and in the shape of the resulting grain size spectrum.

Krüger et al. (1995, henceforth KWS) provided a general computational scheme to describe the evolution of the grain size distribution in one-dimensional stationary flows in consideration of size dependent grain drift. When combined with the well-known equations describing a dust driven wind (given, for example, in Krüger et al. 1994), this multi-component method permits a consistent modeling approach for dust driven winds in consideration of grain drift and yields results different from the preliminary ones of Dominik et al. (1989), once more proving the necessity of self-consistent modeling procedures.

In Sect. 2 we summarize the equations describing the formation and growth of drifting dust grains and our model of a dust driven wind. The computational scheme to calculate the size distribution and the method of solution for the wind model is described in Sect. 3. In Sect. 4 we present representative mod-

Send offprint requests to: D. Krüger

els of stellar winds around C-stars and discuss the influence of grain drift on the shape of the size distribution. The conclusions are given in Sect. 5.

2. Basic equations

For the special case of uniform grain size, i.e. without treating the process of dust growth, the basic equations describing a spherical symmetric, stationary dust driven wind have already been stated in Krüger et al. (1994, henceforth Paper I). We merely list these equations here for sake of completeness and indicate some appropriate modifications made. For further details we refer to Paper I.

Grain formation and growth in consideration of a size dependent drift motion can be described by a special differential form of a balance or conservation equation for the grain size distribution function (KWS). Their equation (15) was appropriately modified and is given in Sect. 2.2 in the context of a stellar outflow.

2.1. Equations for the gas

2.1.1. Conservation of mass, momentum and energy

In the stationary case the equation of continuity can be integrated to give

$$4\pi r^2 \rho_{\rm g} v_{\rm g} = \dot{M} \tag{1}$$

where $\rho_{\rm g}$ and $v_{\rm g}$ are mass density and expansion velocity of the gas, respectively. $\dot{M}$ is the stellar mass loss rate.

The equation of motion for the gas can be cast in the form of a wind equation (Parker 1960)

$$(v_{\rm g}^2 - c_T^2)\frac{{\rm d}v_{\rm g}}{{\rm d}r} = v_{\rm g}\left[\frac{2c_T^2}{r} - \frac{GM_*}{r^2} + \frac{1}{\rho_{\rm g}} f_{\rm drag} - \frac{{\rm d}c_T^2}{{\rm d}r}\right] \tag{2}$$

where p and c_T denote the pressure and isothermal sound velocity of the gas, M_* is the stellar mass and $f_{\rm drag}$ is the collisional drag force exerted on the gas by radiatively accelerated dust grains (cf. Sect. 2.2.4).

In contrast to Paper I, the energy balance of the gas is not treated in detail here. Instead we assume effective radiative relaxation of the bulk of the gas so that the gas temperature $T_{\rm g}$ is given by the radiative equilibrium (RE) temperature $T_{\rm rad}$ defined in Sect. 2.3. As a consequence, the gradient of the squared sound velocity in Eq. (2) is proportional to the gradient of $T_{\rm rad}$ if we assume the variation of the mean molecular weight to be negligible.

A proper inclusion of the gas energy equation would not only obfuscate the influence of grain drift on dust formation and growth but also introduce a stiff component in the resulting large system of ordinary differential equations (cf. Sect. 3) therefore rendering an efficient numerical solution more difficult.

2.1.2. Gas phase chemistry

For simplicity, we assume chemical equilibrium. The concentrations of 25 molecules formed from the elements H, He, O, C, N, Fe, Si, Mg, S, and Al are calculated according to Dominik (1992).

Due to the formation of grains, elements contributing to dust formation and growth are depleted from the gas phase. In case of pure carbon grains the corresponding decrease in the carbon abundance $\epsilon_{\rm C}$ relative to hydrogen is taken into account by the following equation

$$\frac{1}{r^2}\frac{\rm d}{{\rm d}r}\left(r^2 \epsilon_{\rm C} n_{\langle {\rm H}\rangle} v_{\rm g}\right) = -\mathcal{M}_{\rm C} \tag{3}$$

where $n_{\langle {\rm H}\rangle} = n_{\rm H} + 2n_{\rm H_2}$ denotes the total hydrogen density and $\mathcal{M}_{\rm C}$ is the rate of consumption of carbon atoms per volume due to dust growth (cf. Sect. 2.2.4).

Krüger et al. (1996) found that the H/H_2 ratio is a decisive quantity for the determination of the dust growth efficiency (cf. Sect. 2.2.1). In the cooling stellar outflow this ratio will diminish due to H_2 formation via the following reactions

$$3\,{\rm H} \leftrightarrows {\rm H_2} + {\rm H} \tag{4}$$

$$2\,{\rm H} + {\rm H_2} \leftrightarrows 2\,{\rm H_2} \tag{5}$$

$${\rm CH} + {\rm H} \leftrightarrows {\rm C} + {\rm H_2} \tag{6}$$

where the corresponding reaction kinetic data was taken from Millar et al. (1991) and Baulch et al. (1992).

At some point in the CDS, however, the decreasing density and temperature will give rise to a partly frozen chemistry, i.e. all timescales $\tau_{{\rm ch},i}$ of chemical reactions i leading to the formation of H_2 become larger than the hydrodynamical timescale $\tau_{\rm exp} \equiv r/v_{\rm g}$ (cf. Goeres et al. 1988). We therefore extend our chemical equilibrium treatment of the gas phase chemistry by including this important chemical nonequilibrium effect in the following way: In the expanding outflow the H/H_2 ratio is calculated from chemical equilibrium until the condition

$$\sum_{i=1}^{3} \tau_{{\rm ch},i}^{-1} < \tau_{\rm exp}^{-1} \tag{7}$$

is fulfilled at $r = r_{\rm frz}$. For $r > r_{\rm frz}$ the H/H_2 ratio is set equal to that of $r_{\rm frz}$, i.e. the atomic hydrogen concentration is frozen in.

Using the surface reaction rates given in Krüger et al. (1996) we estimated that H_2 formation on grain surfaces always proceeds slowly compared to the hydrodynamical timescale. Thus, the gas phase chemistry is not affected by the grain surface chemistry apart from the carbon consumption due to dust growth (cf. Eq. (3)).

2.2. Equations for the dust

2.2.1. The size evolution of a sample grain

Refraining from discontinuous processes arising, for instance, from grain-grain collisions the size evolution of a spherical grain of radius a in a stationary flow is given by (cf. KWS)

$$\frac{\mathrm{d}a}{\mathrm{d}r} = \frac{1}{v_\mathrm{g} + v_\mathrm{dr}(a)} \frac{1}{\tau_\mathrm{net}(a)} \frac{a_0}{3} \tag{8}$$

where τ_net^{-1} denotes the net rate of grain size change and a_0 is the hypothetical radius of a monomer constituting the grain material (cf. Gail et al. 1984). $v_\mathrm{dr}(a)$ is the drift velocity of a grain of radius a (cf. Sect. 2.2.3). In the following we will refer to the grain radius a as grain 'size' in order to avoid confusion with the independent radial variable r. As can be seen from Eq. (8) grain drift reduces the time available for efficient growth, since the grain is sped up on its trajectory outwards from the star and tends to 'drift away' from the growth region.

We introduce a lower limit a_ℓ of the size of macroscopic particles, thus separating the dust component from the molecular domain and the growth species (cf. Gauger et al. 1990). The value of a_ℓ corresponds to about 10^2 to 10^3 monomers. If a cluster exceeds the size a_ℓ at $r = r_*$ it is considered a newly created dust particle. At radius r such a grain will have grown to a size $a_r(r_*)$ given by integration of Eq. (8)

$$a_r(r_*) = a_\ell + \frac{a_0}{3} \int_{r_*}^{r} \frac{1}{v_\mathrm{g} + v_\mathrm{dr}(a_{r'}(r_*))} \frac{1}{\tau_\mathrm{net}(a_{r'}(r_*))} \mathrm{d}r' . \tag{9}$$

The specific value adopted for a_ℓ has no influence on the outcome of our calculations.

The net rate of grain size change τ_net^{-1} usually comprises contributions from several different physical processes acting on the grain. In this paper, we will consider grain growth and evaporation as well as erosion due to nonthermal sputtering. The net rate is then given by the sum

$$\tau_\mathrm{net}^{-1} = \tau_\mathrm{gr}^{-1} - \tau_\mathrm{ev}^{-1} - \tau_\mathrm{sp}^{-1} \tag{10}$$

where τ_gr and τ_ev denote the characteristic growth and evaporation times, respectively, and τ_sp^{-1} is the nonthermal sputtering rate. We will now discuss each of these contributions in turn.

Grain growth. In CDS of carbon-rich AGB stars the dangling bonds of carbon atoms on a grain surface are expected to be saturated by hydrogen atoms. Growth reactions preferably occur via acetylene addition at temporary radical sites, where an H-atom has been abstracted (dehydrogenation). In a recent paper Krüger et al. (1996, henceforth KPS) argued that the resulting grain material will be amorphous diamond-like carbon, i.e. will have a large proportion of sp^3 bonded carbon. They also devised a method of calculating the dehydrogenation probability p in dependence of the gas and the grain temperature, the H/H_2 ratio and the drift velocity of the grain. According to KPS the grain growth rate can be written as

$$\tau_\mathrm{gr}^{-1} = 4\pi a_0^2 \, 2 n_{\mathrm{C_2H_2}} v_\mathrm{rel}(a) p(a) \tag{11}$$

where $n_{\mathrm{C_2H_2}}$ is the particle density of acetylene and $v_\mathrm{rel}(a)$ is the average relative velocity between the grain and the growth species C_2H_2.

Following Draine (1980) we have used the following approximate expression for the increased average relative velocity due to the drift velocity $v_\mathrm{dr}(a)$ of a grain

$$v_\mathrm{rel}(a) = \left(\mathring{v}_{\mathrm{C_2H_2}}^2 + v_\mathrm{dr}^2(a)/16 \right)^{1/2} . \tag{12}$$

The average relative velocity in the hypothetical case of purely thermal motion (refered to by '$\circ$') is given by

$$\mathring{v}_{\mathrm{C_2H_2}} = \sqrt{\frac{kT_\mathrm{g}}{2\pi m_{\mathrm{C_2H_2}}}} . \tag{13}$$

where $m_{\mathrm{C_2H_2}}$ denotes the mass of an acetylene molecule.

From inspection of Eqs. (11) and (12) it follows that the growth rate may increase significantly if the grain is drifting relative to the gas since the collisional rate between grain and reacting species is increased. Furthermore, KPS showed that p increases for higher relative velocities v_rel since energetic hydrogen atoms colliding with the drifting grain tend to favour the abstraction of hydrogen from the grain surface.

On the other hand, it becomes increasingly difficult for a chemisorbed acetylene molecule to dissipate its surplus translational energy into the lattice, when the relative velocity is high (cf. the discussion in KPS). In order to account for this fact we multiply the growth rate with a sticking efficiency

$$\alpha(v_\mathrm{rel}) = \exp\left[- \left(\frac{0.5 m_{\mathrm{C_2H_2}} v_\mathrm{rel}^2}{4 E_\mathrm{b}} \right)^3 \right] \tag{14}$$

where $E_\mathrm{b} \approx 0.5$ eV can be regarded as a representative value for the binding (or chemisorption) energy of C_2H_2 on sp^3 carbon surfaces (cf. KPS and references therein). The adopted functional dependence of α is suggested by the results of molecular dynamic simulations of van-der-Waals particles (Head-Gordon & Tully 1992) and is also supported by theoretical considerations (cf. KPS and references therein).

In the process of chemisorption of C_2H_2 the triple bond between the two carbon atoms is broken. The resulting structure is then incorporated into the lattice by reconstruction or rearrangement (isomerization) processes and forms a new part of the grain surface. In the case of carbonaceous surfaces this take place on very short timescales from ps to μs (cf. KPS and references therein). At high dust temperatures $T_\mathrm{d} \gtrsim 1600$ K, however, the timescale for desorption of the attached C_2H_2 molecule may be still shorter. In that case, Eq. (11) is no longer applicable and grain growth ceases.

Grain evaporation. At dust temperatures above ~ 1800 K the grain surface is nearly devoid of hydrogen and sublimation takes places through evaporation of C_i chain molecules. According to Lenzuni et al. (1995) the desorption rate is given by

$$\tau_\mathrm{ev}^{-1} = 4\pi a_0^2 \sum_i i \alpha_i \mathring{v}_{\mathrm{C}_i} \frac{p_{\mathrm{sat},i}}{kT_\mathrm{d}} \tag{15}$$

where α_i and $p_{\mathrm{sat},i}$ denote the evaporation coefficient and the vapor saturation pressure over the grain, respectively, of C_i. The corresponding thermodynamic data applicable to amorphous carbon grains are given in Lenzuni et al. (1995). In writing Eq. (15) we have tacitly omitted the term corresponding to the reverse process, i.e. C_i attachment, which can be neglected at the low concentrations of C_i molecules encountered in CDS.

The spontaneous evaporation rate is unaffected by grain drift since it is an intrinsic property of the grain dependent on its internal temperature.

Nonthermal sputtering. As mentioned above, we will also include grain erosion due to nonthermal sputtering, which will become relevant when the drift velocity of a grain exceeds ~ 40 km s^{-1}. The corresponding rate of grain size reduction is given by (cf. also Woitke et al. 1993, KWS)

$$\tau_{\mathrm{sp}}^{-1} = \pi a_0^2 v_{\mathrm{dr}}(a)(n_{\langle \mathrm{H} \rangle} Y_{\mathrm{sp,H}} + n_{\mathrm{He}} Y_{\mathrm{sp,He}}) \tag{16}$$

where $Y_{\mathrm{sp},i}$ denotes the sputtering yield, i.e. the number of lattice particles removed from the grain surface per incident gas particle of species i, and n_i is the number density of that species. In case of solar chemical composition of the gas contributions to the sputtering of carbon grains from elements other than hydrogen and helium can be neglected (Woitke et al. 1993). In our calculation we have used semianalytical yields derived from experimental data (for details see Tielens et al. (1994) and references therein).

2.2.2. The grain size distribution function

According to KWS the value of the grain size distribution $f(a)$ at any radius r and for every grain size $a_r(r_*)$ can be calculated from the following differential balance or conservation equation

$$r^2[v_{\mathrm{g}} + v_{\mathrm{dr}}(a_r(r_*))] f(a_r(r_*)) \frac{\mathrm{d}a_r(r_*)}{\mathrm{d}r_*} + r_*^2 J_\ell(r_*) = 0 \tag{17}$$

where $f(a)$ is the density of grains with size a per size interval $\mathrm{d}a$ and J_ℓ denotes the nucleation rate. For our calculations we adopt the expression for J_ℓ resulting from classical nucleation theory as given by Gail et al. (1984), being aware that the application of classical nucleation theory to grain formation has been critizised, e.g. by Donn & Nuth (1985).

A perhaps more realistic approach is the formulation of the chemical pathway to carbon soot, which proceeds via formation of polycyclic aromatic hydrocarbons (Keller 1987, Frenklach & Feigelson 1989, Cherchneff et al. 1992). We therefore also calculated wind models with a corresponding preliminary nucleation rate (cf. Goeres et al. 1996). However, as these modifications merely resulted in a shift of the condensation zone outwards to larger radii and lower temperatures we will not present these models here.

In writing Eq. (17) we have omitted the source term Q given in KWS which accounts for discontinuous processes arising, for example, from grain-grain collisions. This is most of all due to our poor understanding of the physics of grain-grain collisions (cf. Seab 1987). There seem to be no reaction probabilities or yields available in the literature, the exception being coagulation which has been thoroughly studied by Chokshi et al. (1993). In a recent paper Tielens et al. (1994) also determine the fraction of a grain vaporized by a grain-grain collision. On the other hand, Dominik et al. (1989) have argued that grain coagulation, for instance, is of minor importance in the context of dust driven winds around late-type stars.

The derivative of $a_r(r_*)$ in Eq. (17) is not readily obtained, since $a_r(r_*)$ is actually an integrated quantity (cf. Eq. (9)) depending on $a_{r'}(r_*)$ for $r' < r$. The computational multi-component scheme of KWS comprises the evaluation of $\mathrm{d}a_r(r_*)/\mathrm{d}r_*$ by finite differences on a non-uniform $a_r(r_*)$-grid which is moving in the grain size space. This grid is constructed by following the evolution of the size of a large, variable number of grains originating from appropriately chosen radii $r_i \equiv r_{*,i}$ (cf. Sect. 3).

2.2.3. Velocity and temperature of grains

Concerning the momentum balance of the grains it was shown in Paper I that the grains are closely momentum coupled to the gas and thus move with their respective equilibrium drift velocity relative to the gas. This drift velocity results from balancing $f_{\mathrm{drag}}(a)$, the gravitational force and the radiative acceleration force $f_{\mathrm{rad}}(a)$ acting on a grain of size a and is given by

$$v_{\mathrm{dr}}^2(a) = -\frac{128 c_T^2}{18\pi} + \left[\left(\frac{128 c_T^2}{18\pi} \right)^2 + \left(\frac{4\pi \kappa_H(a) H}{c} - \frac{4\pi G M_* a^3 \rho_{\mathrm{s}}}{3r^2} \right)^2 (\rho_{\mathrm{g}} \pi a^2)^{-2} \right]^{1/2} \tag{18}$$

where ρ_{s} denotes the mass density of the grain material, M_* is the stellar mass, H the frequency integrated Eddington flux (cf. Sect. 2.3) and $\kappa_H(a)$ the corresponding mean absorption cross-section of a single grain.

In order to model the absorption properties of grains we have implemented an approximation similar to that presented by Dominik et al. (1989)

$$\kappa_H(a) = \min \left\{ \pi a^3 \, 5.9 T_{\mathrm{rad}}; 2\pi a^2 \right\}. \tag{19}$$

This expression fits the two limit cases of Mie theory when the grains can be assumed either much smaller or larger than the relevant wavelengths involved (cf. also Paper I).

As has been argued in Paper I the internal lattice temperature T_{d} of the grains is simply given by the RE temperature T_{rad} defined in Sect. 2.3.

2.2.4. Derived quantities

Given the size distribution macroscopic quantities like the total dust opacity κ_H^{d}, the collisional drag force of the grains f_{drag} and the rate of carbon consumption due to grain growth $\mathcal{M}_{\mathrm{C}}$ can

be calculated by simple integration

$$\kappa_H^{\rm d} = \int_{a_\ell}^{\infty} f(a')\kappa_H(a')\,da' \tag{20}$$

$$f_{\rm drag} = f_{\rm rad}^{\rm d} = \frac{4\pi}{c}\kappa_H^{\rm d} H \tag{21}$$

$$\mathscr{M}_{\rm C} = \int_{a_\ell}^{\infty} f(a')\frac{1}{\tau_{\rm net}(a')}\left(\frac{a'}{a_0}\right)^2 da'. \tag{22}$$

2.3. Radiative transfer

Radiative transfer is treated within the framework of a two-stream approximation developed by Lucy (1971) which involves a diluted optical depth variable $\tau_{\rm L}$ defined by

$$\frac{{\rm d}\tau_{\rm L}}{{\rm d}r} = -(\kappa_H^{\rm g} + \kappa_H^{\rm d})\frac{R_*^2}{r^2}. \tag{23}$$

Using the grey approximation the radiative equilibrium temperature is then given by

$$T_{\rm rad}^4 = \frac{T_*^4}{2}\left(1 - \sqrt{1 - \frac{R_*^2}{r^2}} + \frac{3}{2}\tau_{\rm L}\right) \tag{24}$$

and the frequency integrated Eddington flux by

$$H = \frac{\sigma_{\rm R} T_*^4}{4\pi}\left(\frac{R_*}{r}\right)^2. \tag{25}$$

For a more accurate discussion and details on the opacities we refer to Paper I.

3. Method of solution

In the previous section the stellar wind has been described by three ordinary differential equations (ODE's) (2), (3) and (23) for the corresponding quantities $v_{\rm g}$, $\epsilon_{\rm C}$ and $\tau_{\rm L}$. These ODE's are subject to the following boundary conditions

$$\epsilon_{\rm C}(R_*) = \epsilon_{\rm C,0} \tag{26}$$

$$\tau_{\rm L}(R_*) = 2/3 \tag{27}$$

$$\tau_{\rm L}(r \to \infty) = 0 \tag{28}$$

and an additional internal boundary condition to be satisfied at the critical point $r(v_{\rm g} = c_T)$ (cf. Paper I)

$$\frac{2c_T^2}{r} - \frac{GM_*}{r^2} + \frac{1}{\rho_{\rm g}} f_{\rm drag} - \frac{{\rm d}c_T^2}{{\rm d}r} = 0. \tag{29}$$

In order to determine the grain size distribution according to Eq. (17) this system of ODE's is supplemented by a variable number I of ODE's of type (8) for the size evolution of sample grains. The corresponding initial conditions at $r_i \equiv r_{*,i}$ are given by

$$a(r_i) = a_\ell. \tag{30}$$

In this way a moving, non-uniform grid in grain size space is constructed, its points being identified with the momentary size $a_r(r_i)$ of sample grains.

Then, the value of the size distribution at $a_r(r_i)$ for $1 \le i \le I$ can be calculated from Eq. (17) where the derivative ${\rm d}a_r(r_*)/{\rm d}r_*$ is approximated by the analytic derivative of the Lagrange interpolating polynomial of degree two passing through the set of points $\{r_j, a_r(r_j)\}$ with $j = i-1, i, i+1$ (cf. KWS). By appropriate adjustment of the set of points the size distribution at $a_r(r_1)$ and $a_r(r_I)$ can be calculated in an analogous manner.

During the integration of the flow equations outwards from the stellar surface the number I of ODE's of type (8) is successively incremented. This is done in order to achieve a sufficient resolution of the size distribution. A new ODE is added whenever the estimated final size of a grain condensing at the momentary radius r is smaller than a chosen fraction of the estimated final size of the previous sample grain created at r_I:

$$\log a_\infty(r_I) - \log a_\infty(r) > \delta. \tag{31}$$

In the limit case of negligible drift the final grain size can be estimated from the local growth conditions and is given by (Dominik et al. 1989)

$$a_\infty(r) = \tau_{\rm net}^{-1}\frac{a_0}{3}\left(\frac{2v_{\rm g}}{r}\right)^{-1}. \tag{32}$$

The value of δ is chosen according to the desired resolution of the grain size distribution at infinity. In order to get a final number $I_{\rm max}$ of grid points we put

$$\delta = \frac{\log a_\infty(r_1) - \log a_\ell}{I_{\rm max} - 1} \tag{33}$$

corresponding to a roughly logarithmically equidistant grid in grain size space. Numerical experience has shown that $I_{\rm max} \sim 100$ yields a fair resolution, although the code is stable for $I_{\rm max}$ as low as ~ 50. Increasing $I_{\rm max}$ above ~ 300 results in no additional smoothing of the size distribution or its derived quantities.

These derived quantities of the size distribution (cf. Sect. 2.2.4) are calculated by approximating the integrals by the extended trapezoidal rule (cf. KWS).

The combined eigen- and boundary value problem resulting from the ODE's (2), (3), (23) and $I_{\rm max}$ times (8) and their initial or boundary conditions (29), (26), (27), (28) and $I_{\rm max}$ times (30) is solved by the nested shooting method described in Paper I with the following minor modifications made

1. As decscribed above the dimension of the system of ODE's is successively incremented up to $3 + I_{\rm max}$.
2. The free input parameter $a_{\rm d}$ introduced in Paper I is dropped. Dust formation and growth is now treated self-consistently.
3. In the immediate neighbourhood of the critical or sonic point the gradient of the gas velocity is calculated according to l'Hospital's rule.

Table 1. Stellar parameters of Model A and B

	Model A	Model B
L_*	$3\,10^4\,L_\odot$	$5\,10^4\,L_\odot$
T_*	2300 K	2100 K
M_*	$1\,M_\odot$	$1\,M_\odot$
$\epsilon_{\mathrm{C},0}$	$1.7\,\epsilon_{\mathrm{O}}$	$1.7\,\epsilon_{\mathrm{O}}$

Due to our self-consistent modeling approach the mass loss rate has not to be fixed a priori but follows as an eigenvalue of the stellar wind problem.

Since we deal with a large number of $3 + I_{\max}$ non-stiff ODE's the flow equations are solved by means of an embedded, explicit fourth order Runge-Kutta scheme (Hairer et al. 1987). A typical model run needs a few hours of computing time on a Silicon Graphics IRIS Indigo R 4000 workstation.

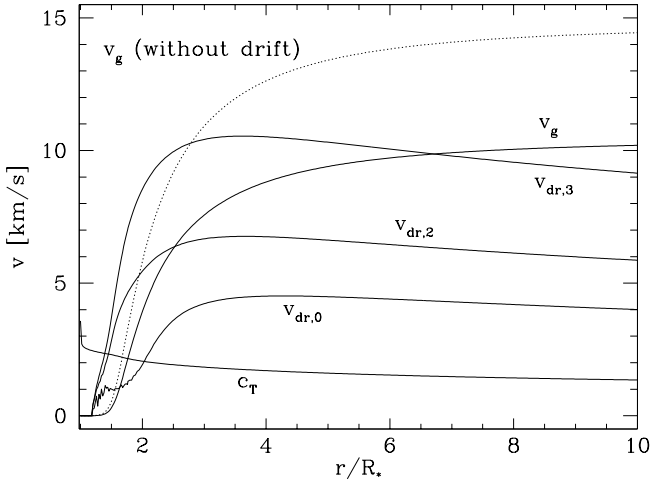

Fig. 1. Dynamical structure of Model A

4. Results and discussion

The multi-component method of KWS for the description of the evolution of the grain size distribution was applied to model spherically symmetric winds around cool carbon stars. We have calculated a grid of models in the domain of purely dust driven winds in the Hertzsprung-Russel diagram (Dominik et al. 1990) varying the values of the stellar parameters lumininosity L_*, effective temperature T_*, and initial carbon abundance $\epsilon_{\mathrm{C},0}$. Our code has proven to be stable for all adopted values of stellar parameters and we thus feel confident that the multi-component method presented by KWS will also work for any other astrophysical context (e.g. accretion flows).

In order to demonstrate the influence of grain drift on the size distribution and its derived integral quantities we present two models of dust driven winds with low and high mass loss rates, respectively. The adopted parameter values are given in Table 1. The initial carbon overabundance of 1.7 is a mean value derived from observations of C-stars (Frantsman & Eglitis 1988). For the chemical abundance of H, He, O, N, Fe, Si, Mg, S and Al solar abundances (Allen 1973) are assumed.

For comparison, each model was recalculated with the drift velocity of the grains artificially set equal to zero.

4.1. Low mass loss model

4.1.1. Structure of the circumstellar envelope

The assumed values of the parameters for Model A which includes grain drift result in a mass loss rate of

$$\dot{M} = 1.5\,10^{-6}\,M_\odot/\mathrm{yr}. \tag{34}$$

The circumstellar dust shell (CDS) is optically thin and thus there is no significant backwarming. The general hydro- and thermodynamical structure is similar to the RE standard model presented in Paper I or by Gail & Sedlmayr (1987). The terminal velocity in Model A reaches $v_{\mathrm{g},\infty} = 10.4\,\mathrm{km\,s^{-1}}$; the maximum ratio of the drag force f_{drag} and the gravitational force $\rho_{\mathrm{g}} g$ is $\alpha_{\max}$=1.6.

The depiction of the grain drift velocity is somewhat difficult, since this drift velocity varies with grain size. We therefore introduce the following mean drift velocities $v_{\mathrm{dr},i}$ defined by

$$v_{\mathrm{dr},i} = \frac{\int_{a_\ell}^{\infty} a^i f(a) v_{\mathrm{dr}}(a)\,da}{\int_{a_\ell}^{\infty} a^i f(a)\,da}. \tag{35}$$

For $i = 0$ Eq. (35) yields the mean drift velocities averaged over all grains. For $i = 1, 2, 3$ the $v_{\mathrm{dr},i}$ can be interpreted as radius, surface or volume weighted drift velocities, respectively. In case of uniform grain composition $v_{\mathrm{dr},3}$ is the drift velocity associated with the center of mass of the dust component.

Fig. 1 depicts the radial course of the sound and expansion velocity of the gas and of the mean drift velocities of the dust. The results of Model A neglecting drift are also plotted and indicated by dashed lines. For increasing i the $v_{\mathrm{dr},i}$ are weighted towards larger grains. The important point to notice here is that although the mean drift velocity $v_{\mathrm{dr},0}$ is of moderate magnitude and comparable with the thermal sound velocity of the gas the bulk of the dust moves with a drift velocity $v_{\mathrm{dr},3}$ relative to the gas which is of the same order as the gas velocity. In the inner region of the wind $v_{\mathrm{dr},3}$ may even be much higher than the gas velocity.

4.1.2. Grain size distribution

The formation or temporal evolution of the size distribution f in dust driven winds has been discussed in detail by Dominik et al. (1989) for the limit case of neglected drift. Their main results remain valid and will be shortly summarized here

– In the inner, subsonic region the growth conditions are excellent. Moreover, the grains remain in this region for a long time. As later growth further downstream is negligible the grains grow to a large final size almost locally. However, due to comparatively high temperatures close to the star only few

grains are formed resulting in the characteristic tail of the distribution function for very large grain sizes.
- In the sonic point region nucleation is very efficient. Most of the grains are created here. They are of medium size since growth conditions have deteriorated due to decreasing gas density and reduced hydrodynamical time scale.
- In the outer, supersonic region the wind becomes increasingly diluted and after some further growth of existing grains the size distribution rapidly approaches the final distribution. Only few new grains are created which do not grow efficiently and form the tail of the size distribution for very small grains.

We will now turn to a discussion of how the consideration of grain drift affects the final size distribution. There are five main effects of drift

- Since the flux of grains is conserved the dust becomes increasingly dynamically diluted for high drift velocities (cf. Eq. (17) and Paper I).
- The collisional rate between grain and growth species is increased due to larger relative velocities (cf. Eq. (12)).
- The dehydrogenation probability p increases, since the activation energy barrier for hydrogen–abstraction is overcome more easily (cf. KPS).
- For drift velocities exceeding $\sim 5\,\mathrm{km\,s^{-1}}$ the growth species tends to just bounce off the grain surface, i.e. the sticking efficiency α decreases (cf. Eq. (14)).
- As the grain drifts out of the gas element where it has been created, the time of residence in a region of efficient growth is reduced (cf. Eq. (8)).

The four latter effects directly influence the growth efficiency of dust grains.

We introduce a quantity A_i defined by

$$A_i = \left(1 + \left(\frac{v_{\mathrm{dr},i}}{4\mathring{v}_{\mathrm{C_2H_2}}}\right)^2\right)^{1/2} \cdot \frac{p(v_{\mathrm{dr},i})}{p} \cdot \alpha(v_{\mathrm{dr},i}) \cdot \frac{v_{\mathrm{g}}}{v_{\mathrm{g}} + v_{\mathrm{dr},i}} \tag{36}$$

as a measure of the modification of the local growth rate, such that A_i comprises all four effects. Here, $p(v_{\mathrm{dr},i})$ and $\alpha(v_{\mathrm{dr},i})$ are calculated for relative velocities v_{rel}, which are increased according to drift velocities $v_{\mathrm{dr},i}$, while p is calculated for the hypothetical case of purely thermal relative motion. Each of the four factors in Eq. (36) corresponds to one of the effects mentioned above: the 'sweeping up' of condensable material, the increased surface density of radical sites, the reduced sticking efficiency and the 'drifting away'. Again, for increasing i the A_i correspond to increasingly larger grains.

Fig. 2 depicts the radial course of A_i for $i = 0, 2, 3$. In the subsonic regime close to the star the growth efficiency is depressed by a factor of up to 10^2, since the grain velocity, though small compared to the sound velocity, is much larger than the expansion velocity of the gas and grains quickly drift away from their point of creation outwards to regions of less efficient growth.

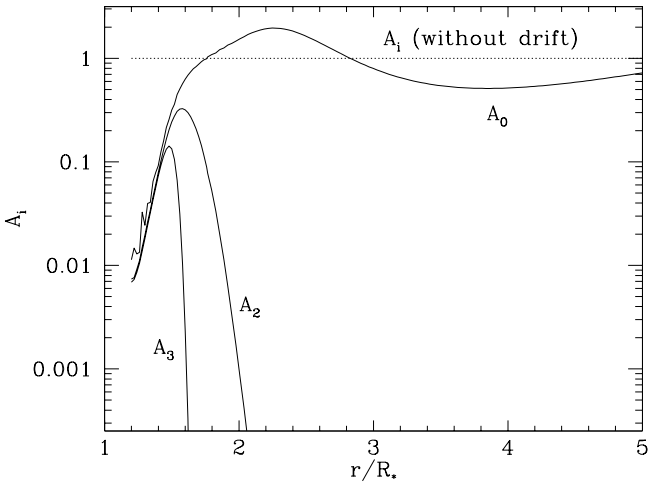

Fig. 2. Relative change A_0, A_2, A_3 of local growth rate due to drift velocities $v_{\mathrm{dr},0}, v_{\mathrm{dr},2}, v_{\mathrm{dr},3}$ for Model A

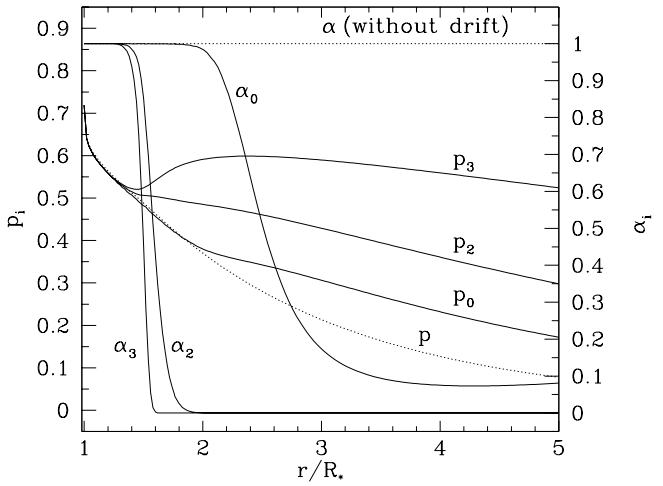

Fig. 3. Dehydrogenation probability $p_i \equiv p(v_{\mathrm{dr},i})$ and sticking efficiency $\alpha_i \equiv \alpha(v_{\mathrm{dr},i})$ for Model A. Dashed lines indicate the resulting p, α neglecting drift

The majority of the grains is created around the sonic point. Here, the two drift effects of 'sweeping up' and 'drifting away' approximately cancel for these small grains ($a \sim 10$ nm). There is, however, no further growth of large or medium sized grains: Although the large drift velocity of these grains somewhat increases their surface radical density, the sticking efficiency α_3 is virtually zero (cf. Fig. 3). In the outer region ($r \gtrsim 4\,R_*$) grain drift continues to inhibit further growth of large grains and somewhat reduces the growth efficiency of small grains.

The resulting size distribution at $r = 30\,R_*$ is shown in the upper panel of Fig. 4. The dashed line included for comparison indicates the model with zero drift velocity. By comparison, the size distribution corresponding to the model including grain drift appears distorted. There is a pronounced decrease of the distribution at small grain sizes (1 nm $< a <$ 10 nm).

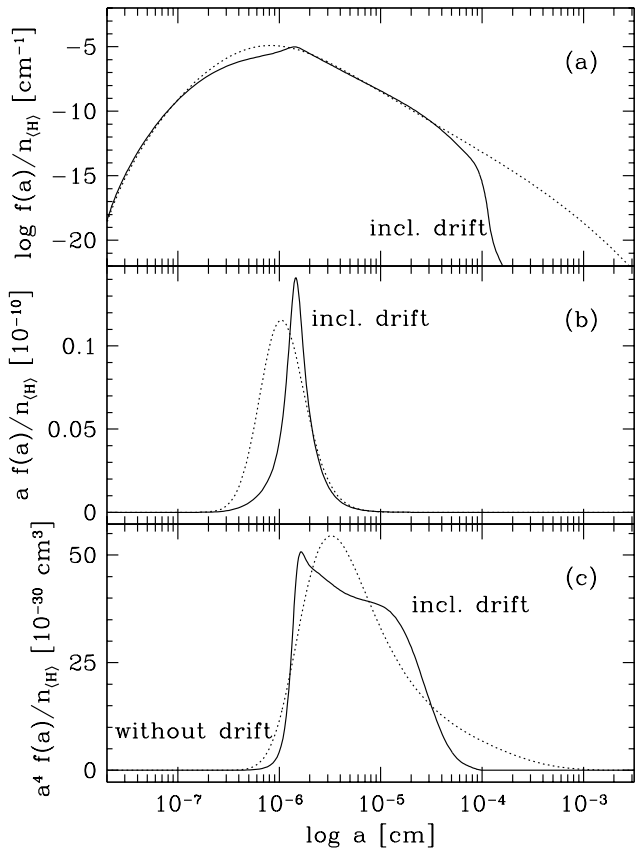

Fig. 4. a Grain size distribution for Model A. **b** Size distribution multiplied by a. **c** Size distribution multiplied by a^4. All quantities are normated to the total hydrogen density

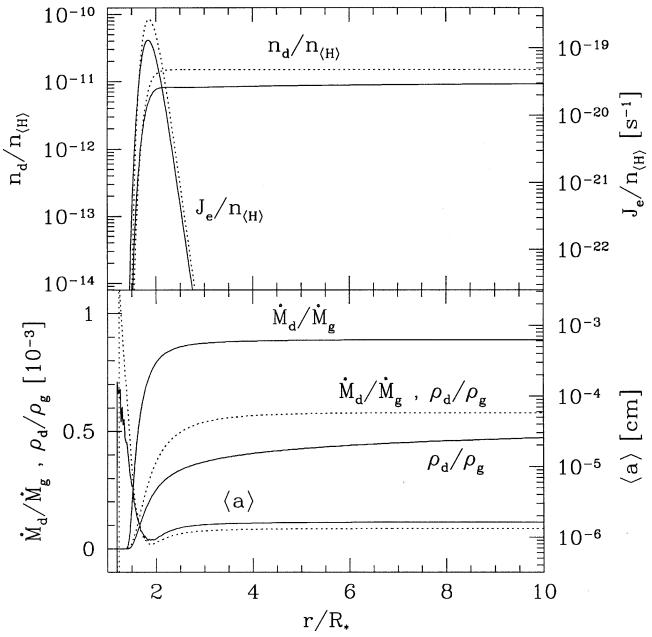

Fig. 5. Radial course of dust related quantities for Model A. Dashed lines indicate the results neglecting drift

The cut-off of the distribution function at $a \sim 1$ μm is mainly due nonthermal sputtering. Grains larger than this limit size have very high drift velocities ($v_{\rm dr}(a) \gtrsim 40\,{\rm km\,s^{-1}}$) and are efficiently eroded by collisions with gas particles (mainly He atoms). This cut-off of the distribution function has also been postulated by Jura (1994) in order to explain the observed circumstellar polarisation of IRC+10216 at 2.2 μm (K-band).

To first order, both distribution functions can be fitted piecewise by power laws of the form a^γ. The spectral indices for the descending branches of the distribution functions (which make up most of the mass of the dust component, see below) are $\gamma \approx -4.2$ for the model where drift was included and $\gamma \approx -4.6$ when drift is neglected. Though tempting in this context, we think it is not apt to compare the obtained spectral indices with the one deduced for the grain size spectrum in the interstellar medium (Mathis et al. 1977) which is $\gamma \sim -3.5$. The latter is bound to result from the superposition of many size distributions originating from distinct dust forming objects, and is furthermore subject to constant processing by interstellar shock waves (e.g. Liffman & Clayton 1989).

We also present plots of $f(a)$ multiplied by a and a^4. In Fig. 4b the area below the curve for a given size interval $\Delta \log a$ now corresponds to the *number* of grains in this interval. Obviously, without drift the total number of grains is higher than in the case where drift is included, although the position of the maximum, i. e. the most probable or mean grain radius, varies only little. This can also be seen from the radial course of the macroscopic quantities (cf. Fig. 5). Depicted are the nucleation rate J_ℓ and the corresponding increase of the number density $n_{\rm d}$ of dust grains, both normated to the total hydrogen density. The lower panel shows the ratio $\dot{M}_{\rm d}/\dot{M}_{\rm g}$ of the mass loss rates of the dust and the gas component, the corresponding mass density ratio $\rho_{\rm d}/\rho_{\rm g}$, which is equal to $\dot{M}_{\rm d}/\dot{M}_{\rm g}$ only in case of negligible drift, and the mean grain radius $\langle a \rangle$.

This reduction of the grain density due to drift by about 40% can be explained in the following way: First, the dust component is dynamically diluted. Furthermore, there are less grains created in the first place, i.e. the nucleation rate peaks at a lower value. This is due to the fact that comparatively many large grains are formed in the inner region consuming a significant portion of condensable material (and therefore suppressing further efficient nucleation) without efficiently driving the wind (since these grains are dynamically diluted). This effect of drift should be quite independent of the specific nucleation mechanism adopted here, since every realistic expression for the nucleation rate will to *some* degree be dependent on the amount of condensable material.

In Fig. 4c the area below the curve corresponds to the *volume* or *mass* contained in the grains. The consideration of drift leads to a considerable distortion of the distribution of condensed matter. The average grain mass is now 40% larger as in the case of neglected drift. Although $n_{\rm d}$ is reduced, the dust-to-gas mass ratio $\dot{M}_{\rm d}/\dot{M}_{\rm g}$ injected into the ISM, is increased by about 50% compared to the case of neglected drift (cf. the lower panel of Fig. 5). On the other hand, the dust component is dynamically

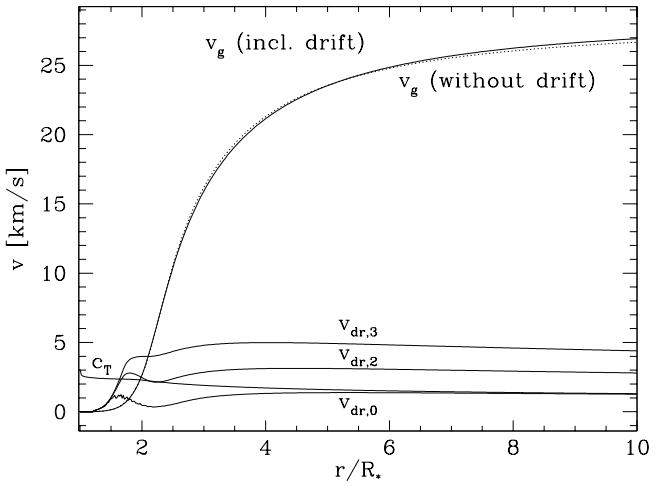

Fig. 6. Dynamical structure for Model B

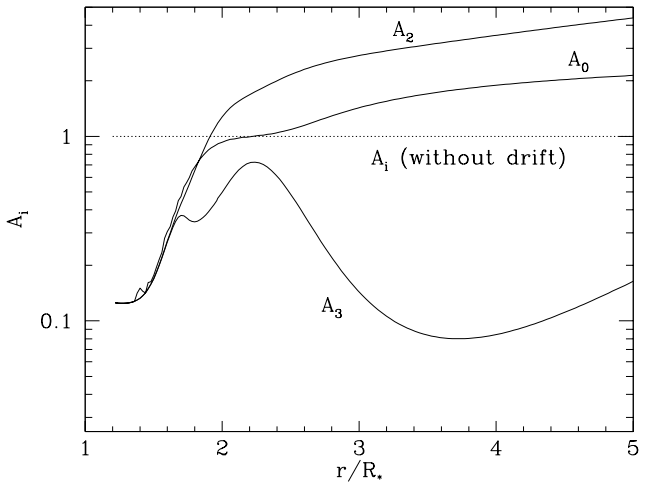

Fig. 7. Relative change A_0, A_2, A_3 of local growth rate due to drift velocities $v_{\rm dr,0}, v_{\rm dr,2}, v_{\rm dr,3}$ for Model B

diluted due to the drift increased terminal velocity of the grains and the overall mass density $\rho_{\rm d}$ actually decreases somewhat (cf. Fig. 5).

In this context, we would like to emphasize that the commonly employed method of determining $\dot{M}_{\rm d}$ (e.g. Knapp 1985, Jura 1986) has to be used with care. This has already been noted by Sahai (1990) and Olofsson et al. (1993). In fitting the observed IR-flux of the dust by simple radiative transfer models it is often assumed that the dust velocity is equal to the expansion velocity of the gas. In fact, this procedure only yields the diluted dust density $\rho_{\rm d}$ and misses a factor of $(v_{\rm g} + v_{\rm dr,3})/v_{\rm g}$.

From Fig. 4 it can furthermore be seen that grain erosion due to nonthermal sputtering has only a minor influence on the dust component as a whole. The majority of the grains simply is not affected, since they are smaller than the cut-off size (cf. Fig. 4b). Only the largest of the mass-bearing grains are subject to sputtering resulting in the comparatively steep right flank of the size distribution in Fig. 4a.

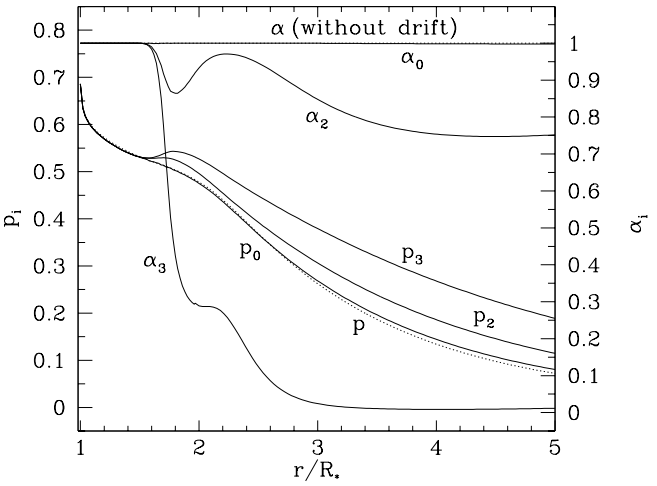

Fig. 8. Dehydrogenation probability $p_i \equiv p(v_{{\rm dr},i})$ and sticking efficiency $\alpha_i \equiv \alpha(v_{{\rm dr},i})$ for Model B. Dashed lines indicate the resulting p, α neglecting drift

4.2. High mass loss model

4.2.1. Structure of the circumstellar envelope

The parameters assumed for Model B including grain drift result in a mass loss rate of

$$\dot{M} = 5.5\,10^{-5}\,M_\odot/{\rm yr}. \tag{37}$$

The circumstellar dust shell is optically thick and gives rise to substantial backwarming. The general hydro- and thermodynamical structure is similar to the RE standard model presented in Paper I or by Gail & Sedlmayr (1987). The terminal velocity of Model B reaches $v_{{\rm g},\infty} = 28.3\,{\rm km\,s^{-1}}$; the maximum ratio of the drag force $f_{\rm drag}$ and the gravitational force $\rho_{\rm g} g$ is $\alpha_{\rm max}$=11.2.

Fig. 6 depicts the radial course of the sound and expansion velocity of the gas and of the mean drift velocities of the dust. The results of Model B neglecting drift are also plotted and indicated by dashed lines. Due to higher gas densities in Model B compared to Model A the drift velocities are reduced to values $\lesssim 5\ {\rm km\ s^{-1}}$. However, in the inner region of the wind the grains still move significantly faster than the gas.

4.2.2. Grain size distribution

Fig. 7 depicts the radial course of A_i for $i = 0, 2, 3$. For the high mass loss Model B the growth efficiency is depressed only by a factor of up to 8 in the subsonic regime which is much less than in Model A. In the outer region ($r > 3\,R_*$) growth is enhanced by a factor of up to 4 for the small and medium size grains due to the enhanced dehydrogenation probability of the carbonaceous grain surface (cf. Fig. 8) and the 'sweeping up' of condensable material. As in model A, the sticking efficiency α_3 of the growth species on large grains is small beyond the sonic point, and there is little further growth of these grains.

The resulting size distribution at $r = 30\,R_*$ is shown in the upper panel of Fig. 9. The dashed line indicates the model with

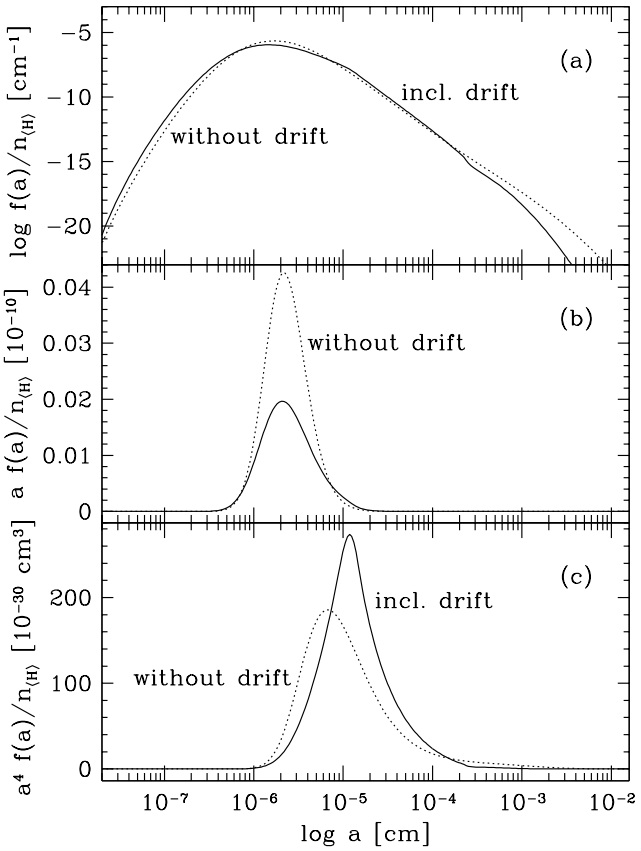

Fig. 9. a Grain size distribution for Model B. **b** Size distribution multiplied by a. **c** Size distribution multiplied by a^4. All quantities are normated to the total hydrogen density

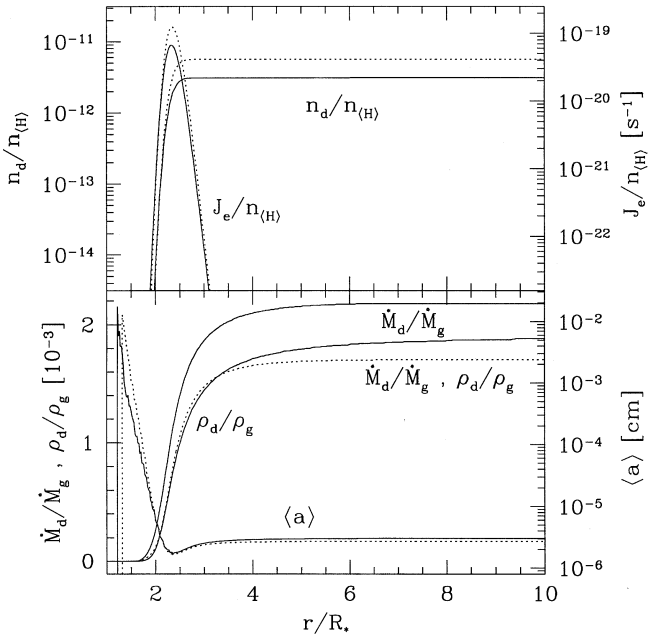

Fig. 10. Radial course of dust related quantities for Model B. Dashed lines indicate the results neglecting drift

zero drift velocity included for comparison. The consideration of drift now leads to a less significant distortion of the size distribution. However, the amount of ultrasmall particles ($a \lesssim 10$ Å) is increased by nearly an order of magnitude. The existence of such an ultrasmall grain component in the ISM has been suggested on the ground of observations of 1–25 μm infrared emission from interstellar clouds (Sellgren et al. 1983).

The relevant part of the size distribution of Model B including drift can be fitted by power laws with spectral indices $\gamma_1 \approx -2.6\,(20\,\mathrm{nm} < a < 0.1\mu\mathrm{m})$ and $\gamma_2 \approx -5.3\,(a > 0.1\mu\mathrm{m})$, respectively. In the case where drift was neglected the descending branch of the distribution function obeys a power law of the form $a^{-5.1}$.

In analogy to the low mass loss Model A the grain density is reduced by a factor of almost 2 (cf. Figs. 9b and 10) compared to the case of neglected drift for the same reasons as given in Sect. 4.1.2.

The distribution of condensed material is shifted towards larger grains (cf. Fig. 9c). The average grain mass is twice as large, and the relative mass loss rate $\dot{M}_\mathrm{d}/\dot{M}_\mathrm{g}$ of the dust component is raised by about 30% compared to the case of neglected drift (cf. Fig. 10). Furthermore, although n_d is reduced, the overall mass density ρ_d of the dust component also somewhat increases (cf. the lower panel of Fig. 10).

Because of the moderate drift velocities in Model B nonthermal sputtering has no influence on the shape of the grain size spectrum.

5. Conclusions

By means of the multi-component method of KWS we have constructed self-consistent models of dust driven winds in consideration of a size dependent grain drift and growth rate, determining for the first time the shape of the corresponding grain size spectrum. It turned out that although the consideration of grain drift does not greatly affect the resulting general hydro- and thermodynamical structure of the circumstellar envelope it has an decisive influence on the resulting grain size spectrum.

Generally, less but more massive grains are being formed in the models where drift is included. These results are contrary to the preliminary ones obtained by Dominik et al. (1989).

Concerning microscopic processes, drift mainly reduces the sticking efficiency of the growth species acetylene on large grains with significant drift velocities, although for carbon grains the surface density of radical sites is somewhat increased. Nonthermal sputtering is relevant only for very large grains ($a \gtrsim 1\mu$m) in tenuous winds ($\dot{M} \lesssim 10^{-6}\,M_\odot/\mathrm{yr}$).

With regard to stellar diagnostics, grain drift directly affects the prediction of the amount $\dot{M}_\mathrm{d}$ of dust injected into the interstellar medium. Concerning the modeling of dust driven winds, characteristic quantities like the mass and number density ratio of dust and gas are affected when compared to one-fluid models. The modeling of the optical appearance of circumstellar dust shells should also benefit from a proper consideration of

drift, since the resulting spectra depend on the specific shape of the grain size distribution.

The influence of drift gradually increases with decreasing mass loss rate, i.e. decreasing density in the CDS. Thus, the consideration of drift seems to be especially important for our correct understanding of those objects with low to moderate mass loss rates up to about $10^{-5}\,M_{\odot}$/yr.

Acknowledgements. D. Krüger would like to thank the referee A. G. G. M. Tielens for inspiring comments on the manuscript. Thanks also to P. Woitke for helpful discussions and to J. M. Winters and A. B. C. Patzer for a critical reading of the manuscript.

References

Allen C. W., 1973, *Astrophysical Quantities*, The Athlone Press, London
Baulch D. L., Cobos C. J., Cox R. A. et al., 1992, J. Phys. Chem. Ref. Data 21, 411
Beck H. K. B., Gail H.-P., Henkel R., Sedlmayr E., 1992, A&A 265, 626
Bowen G. H., 1988, ApJ 329, 299
Cherchneff I., Barker J. R., Tielens A. G. G. M., 1992, ApJ 401, 269
Chokshi A., Tielens A. G. G. M., Hollenbach D., 1993, ApJ 407, 806
Dominik C., 1992, *Formation of dust grains in the winds of cool giants*, PhD thesis, Technische Universität, Berlin, FRG
Dominik C., Gail H.-P., Sedlmayr E., 1989, A&A 223, 227
Dominik C., Gail H.-P., Sedlmayr E., Winters J. M., 1990, A&A 240, 365
Donn B., Nuth J. A., 1985, ApJ 288, 187
Draine B. T., 1980, ApJ 241, 1021
Fleischer A. J., Gauger A., Sedlmayr E., 1992, A&A 266, 321
Frantsman Y. L., Eglitis I. E., 1988, SvA 14, L109
Frenklach M., Feigelson E. D., 1989, ApJ 341, 372
Gail H.-P., Sedlmayr E., 1987, A&A 171, 197
Gail H.-P., Sedlmayr E., 1988, A&A 206, 153
Gail H.-P., Keller R., Sedlmayr E., 1984, A&A 133, 320
Gauger A., Gail H.-P., Sedlmayr E., 1990, A&A 235, 345
Goeres A., Henkel R., Sedlmayr E., Gail H.-P., 1988, Rev.Mod.Astron. 1, 231
Goeres A., Keller R., Sedlmayr E., Gail H.-P., 1996, Polycyclic Aromatic Compounds 8, 129
Hairer E., Nørsett S. P., Wanner G., 1987, *Solving Ordinary Differential Equations I*, Springer, Berlin
Head-Gordon M., Tully J. C., 1992, Surf. Sci. 268, 113
Jura M., 1986, ApJ 303, 327
Jura M., 1994, ApJ 434, 713
Keller R., 1987, In Léger A., d'Hendecourt L., Boccara N., *Polycyclic Aromatic Hydrocarbons and Astrophysics*, 387. Reidel Publ. Comp.
Knapp G. R., 1985, ApJ 293, 273
Kozasa T., Hasegawa H., Seki J., 1984, Ap&SS 98, 61
Krüger D., Gauger A., Sedlmayr E., 1994, A&A 290, 573 (paper I)
Krüger D., Woitke P., Sedlmayr E., 1995, A&AS 113, 593 (KWS)
Krüger D., Patzer A. B. C., Sedlmayr E., 1996, A&A 313, 891 (KPS)
Kwok S., 1975, ApJ 198, 583
Lafon J.-P., Berruyer N., 1991, A&AR 2, 249
Lenzuni P., Gail H.-P., Henning T., 1995, ApJ 447, 848
Liffman K., Clayton D. D., 1989, ApJ 340, 853
Lucy L. B., 1971, ApJ 163, 95
MacGregor K. B., Stencel R. E., 1992, ApJ 397, 644
Mathis J. S., Rumpl W., Nordsieck K. H., 1977, ApJ 217, 425
Millar T. J., Rawlings J. M. C., Bennett A., Brown P. D., Charnley S. B., 1991, A&AS 87, 585
Nejad L. A. M., Millar T. J., 1987, A&A 183, 279
Netzer N., Elitzur M., 1993, ApJ 410, 701
Olofsson H., Eriksson K., Gustafsson B., Carlström U., 1993, ApJS 87, 267
Parker E. N., 1960, ApJ 132, 175
Rowan-Robinson M., Harris S., 1982, MNRAS 200, 197
Sahai R., 1990, ApJ 362, 652
Seab C. G., 1987, In Hollenbach D. J., Thronson H. A., Jr., *Interstellar processes*, 491, D. Reidel, Dordrecht
Sedlmayr E., Dominik C., 1995, Space Sci. Rev. 73, 211
Sellgren K., Werner M. W., Dinerstein H. L., 1983, ApJ 271, L13
Tielens A. G. G. M., 1983, ApJ 271, 702
Tielens A. G. G. M., McKee C. F., Seab C. G., Hollenbach D. J., 1994, ApJ 431, 321
Winters J. M., Dominik C., Sedlmayr E., 1994, A&A 288, 255
Woitke P., Dominik C., Sedlmayr E., 1993, A&A 274, 451

This article was processed by the author using Springer-Verlag LaTeX A&A style file *L-AA* version 3.